Valparaiso University

ValpoScholar

Physics and Astronomy Faculty Publications

Department of Physics and Astronomy

9-10-2016

Jet-like Correlations with Direct-Photon and Neutral-Pion Triggers at sNN=200 GeV

Adam Gibson-Even

Valparaiso University, Adam.Gibson-Even@valpo.edu

Follow this and additional works at: http://scholar.valpo.edu/phys_astro_fac_pub

Jet-like correlations with direct-photon and neutral-pion triggers at $\sqrt{s_{NN}} = 200$ GeV

CrossMark

STAR Collaboration

L. Adamczyk [a], J.K. Adkins [t], G. Agakishiev [r], M.M. Aggarwal [af], Z. Ahammed [aw], I. Alekseev [p], D.M. Anderson [aq], A. Aparin [r], D. Arkhipkin [c], E.C. Aschenauer [c], M.U. Ashraf [at], A. Attri [af], G.S. Averichev [r], X. Bai [g], V. Bairathi [ac], R. Bellwied [as], A. Bhasin [q], A.K. Bhati [af], P. Bhattarai [ar], J. Bielcik [j], J. Bielcikova [k], L.C. Bland [c], I.G. Bordyuzhin [p], J. Bouchet [s], J.D. Brandenburg [ak], A.V. Brandin [ab], I. Bunzarov [r], J. Butterworth [ak], H. Caines [ba], M. Calderón de la Barca Sánchez [e], J.M. Campbell [ad], D. Cebra [e], I. Chakaberia [c], P. Chaloupka [j], Z. Chang [aq], A. Chatterjee [aw], S. Chattopadhyay [aw], X. Chen [w], J.H. Chen [an], J. Cheng [at], M. Cherney [i], W. Christie [c], G. Contin [x], H.J. Crawford [d], S. Das [m], L.C. De Silva [i], R.R. Debbe [c], T.G. Dedovich [r], J. Deng [am], A.A. Derevschikov [ah], B. di Ruzza [c], L. Didenko [c], C. Dilks [ag], X. Dong [x], J.L. Drachenberg [v], J.E. Draper [e], C.M. Du [w], L.E. Dunkelberger [f], J.C. Dunlop [c], L.G. Efimov [r], J. Engelage [d], G. Eppley [ak], R. Esha [f], O. Evdokimov [h], O. Eyser [c], R. Fatemi [t], S. Fazio [c], P. Federic [k], J. Fedorisin [r], Z. Feng [g], P. Filip [r], Y. Fisyak [c], C.E. Flores [e], L. Fulek [a], C.A. Gagliardi [aq], D. Garand [ai], F. Geurts [ak], A. Gibson [av], M. Girard [ax], L. Greiner [x], D. Grosnick [av], D.S. Gunarathne [ap], Y. Guo [al], S. Gupta [q], A. Gupta [q], W. Guryn [c], A.I. Hamad [s], A. Hamed [aq], R. Haque [ac], J.W. Harris [ba], L. He [ai], S. Heppelmann [ag], S. Heppelmann [e], A. Hirsch [ai], G.W. Hoffmann [ar], S. Horvat [ba], T. Huang [bb], B. Huang [h], X. Huang [at], H.Z. Huang [f], P. Huck [g], T.J. Humanic [ad], G. Igo [f], W.W. Jacobs [o], H. Jang [u], A. Jentsch [ar], J. Jia [c], K. Jiang [al], E.G. Judd [d], S. Kabana [s], D. Kalinkin [o], K. Kang [at], K. Kauder [ay], H.W. Ke [c], D. Keane [s], A. Kechechyan [r], Z.H. Khan [h], D.P. Kikoła [ax], I. Kisel [l], A. Kisiel [ax], L. Kochenda [ab], D.D. Koetke [av], L.K. Kosarzewski [ax], A.F. Kraishan [ap], P. Kravtsov [ab], K. Krueger [b], L. Kumar [af], M.A.C. Lamont [c], J.M. Landgraf [c], K.D. Landry [f], J. Lauret [c], A. Lebedev [c], R. Lednicky [r], J.H. Lee [c], X. Li [al], Y. Li [at], C. Li [al], W. Li [an], X. Li [ap], T. Lin [o], M.A. Lisa [ad], F. Liu [g], Y. Liu [aq], T. Ljubicic [c], W.J. Llope [ay], M. Lomnitz [s], R.S. Longacre [c], X. Luo [g], S. Luo [h], G.L. Ma [an], L. Ma [an], Y.G. Ma [an], R. Ma [c], N. Magdy [ao], R. Majka [ba], A. Manion [x], S. Margetis [s], C. Markert [ar], H.S. Matis [x], D. McDonald [as], S. McKinzie [x], K. Meehan [e], J.C. Mei [am], Z.W. Miller [h], N.G. Minaev [ah], S. Mioduszewski [aq], D. Mishra [ac], B. Mohanty [ac], M.M. Mondal [aq], D.A. Morozov [ah], M.K. Mustafa [x], B.K. Nandi [n], Md. Nasim [f], T.K. Nayak [aw], G. Nigmatkulov [ab], T. Niida [ay], L.V. Nogach [ah], S.Y. Noh [u], J. Novak [aa], S.B. Nurushev [ah], G. Odyniec [x], A. Ogawa [c], K. Oh [aj], V.A. Okorokov [ab], D. Olvitt Jr. [ap], B.S. Page [c], R. Pak [c], Y.X. Pan [f], Y. Pandit [h], Y. Panebratsev [r], B. Pawlik [ae], H. Pei [g], C. Perkins [d], P. Pile [c], J. Pluta [ax], K. Poniatowska [ax], J. Porter [x], M. Posik [ap], A.M. Poskanzer [x], N.K. Pruthi [af], M. Przybycien [a], J. Putschke [ay], H. Qiu [x], A. Quintero [s],

S. Ramachandran [t], R.L. Ray [ar], R. Reed [y], H.G. Ritter [x], J.B. Roberts [ak], O.V. Rogachevskiy [r], J.L. Romero [e], L. Ruan [c], J. Rusnak [k], O. Rusnakova [j], N.R. Sahoo [aq,*], P.K. Sahu [m], I. Sakrejda [x], S. Salur [x], J. Sandweiss [ba], A. Sarkar [n], J. Schambach [ar], R.P. Scharenberg [ai], A.M. Schmah [x], W.B. Schmidke [c], N. Schmitz [z], J. Seger [i], P. Seyboth [z], N. Shah [an], E. Shahaliev [r], P.V. Shanmuganathan [s], M. Shao [al], A. Sharma [q], B. Sharma [af], M.K. Sharma [q], W.Q. Shen [an], Z. Shi [x], S.S. Shi [g], Q.Y. Shou [an], E.P. Sichtermann [x], R. Sikora [a], M. Simko [k], S. Singha [s], M.J. Skoby [o], D. Smirnov [c], N. Smirnov [ba], W. Solyst [o], L. Song [as], P. Sorensen [c], H.M. Spinka [b], B. Srivastava [ai], T.D.S. Stanislaus [av], M. Stepanov [ai], R. Stock [l], M. Strikhanov [ab], B. Stringfellow [ai], M. Sumbera [k], B. Summa [ag], Y. Sun [al], Z. Sun [w], X.M. Sun [g], B. Surrow [ap], D.N. Svirida [p], Z. Tang [al], A.H. Tang [c], T. Tarnowsky [aa], A. Tawfik [az], J. Thäder [x], J.H. Thomas [x], A.R. Timmins [as], D. Tlusty [ak], T. Todoroki [c], M. Tokarev [r], S. Trentalange [f], R.E. Tribble [aq], P. Tribedy [c], S.K. Tripathy [m], O.D. Tsai [f], T. Ullrich [c], D.G. Underwood [b], I. Upsal [ad], G. Van Buren [c], G. van Nieuwenhuizen [c], M. Vandenbroucke [ap], R. Varma [n], A.N. Vasiliev [ah], R. Vertesi [k], F. Videbæk [c], S. Vokal [r], S.A. Voloshin [ay], A. Vossen [o], H. Wang [c], F. Wang [ai], Y. Wang [g], J.S. Wang [w], G. Wang [f], Y. Wang [at], J.C. Webb [c], G. Webb [c], L. Wen [f], G.D. Westfall [aa], H. Wieman [x], S.W. Wissink [o], R. Witt [au], Y. Wu [s], Z.G. Xiao [at], W. Xie [ai], G. Xie [al], K. Xin [ak], N. Xu [x], Q.H. Xu [am], Z. Xu [c], J. Xu [g], H. Xu [w], Y.F. Xu [an], S. Yang [al], Y. Yang [g], C. Yang [al], Y. Yang [w], Y. Yang [bb], Q. Yang [al], Z. Ye [h], Z. Ye [h], L. Yi [ba], K. Yip [c], I.-K. Yoo [aj], N. Yu [g], H. Zbroszczyk [ax], W. Zha [al], Z. Zhang [an], J.B. Zhang [g], S. Zhang [an], S. Zhang [al], X.P. Zhang [at], Y. Zhang [al], J. Zhang [w], J. Zhang [am], J. Zhao [ai], C. Zhong [an], L. Zhou [al], X. Zhu [at], Y. Zoulkarneeva [r], M. Zyzak [l]

[a] *AGH University of Science and Technology, FPACS, Cracow 30-059, Poland*
[b] *Argonne National Laboratory, Argonne, IL 60439, United States*
[c] *Brookhaven National Laboratory, Upton, NY 11973, United States*
[d] *University of California, Berkeley, CA 94720, United States*
[e] *University of California, Davis, CA 95616, United States*
[f] *University of California, Los Angeles, CA 90095, United States*
[g] *Central China Normal University, Wuhan, Hubei 430079, China*
[h] *University of Illinois at Chicago, Chicago, IL 60607, United States*
[i] *Creighton University, Omaha, NE 68178, United States*
[j] *Czech Technical University in Prague, FNSPE, Prague 115 19, Czech Republic*
[k] *Nuclear Physics Institute AS CR, 250 68 Prague, Czech Republic*
[l] *Frankfurt Institute for Advanced Studies FIAS, Frankfurt 60438, Germany*
[m] *Institute of Physics, Bhubaneswar 751005, India*
[n] *Indian Institute of Technology, Mumbai 400076, India*
[o] *Indiana University, Bloomington, IN 47408, United States*
[p] *Alikhanov Institute for Theoretical and Experimental Physics, Moscow 117218, Russia*
[q] *University of Jammu, Jammu 180001, India*
[r] *Joint Institute for Nuclear Research, Dubna 141 980, Russia*
[s] *Kent State University, Kent, OH 44242, United States*
[t] *University of Kentucky, Lexington, KY 40506-0055, United States*
[u] *Korea Institute of Science and Technology Information, Daejeon 305-701, Republic of Korea*
[v] *Lamar University, Beaumont, TX 77710, United States*
[w] *Institute of Modern Physics, Chinese Academy of Sciences, Lanzhou, Gansu 730000, China*
[x] *Lawrence Berkeley National Laboratory, Berkeley, CA 94720, United States*
[y] *Lehigh University, Bethlehem, PA 18015, United States*
[z] *Max-Planck-Institut fur Physik, Munich 80805, Germany*
[aa] *Michigan State University, East Lansing, MI 48824, United States*
[ab] *National Research Nuclear University MEPhI, Moscow 115409, Russia*
[ac] *National Institute of Science Education and Research, Bhubaneswar 751005, India*
[ad] *Ohio State University, Columbus, OH 43210, United States*
[ae] *Institute of Nuclear Physics PAN, Cracow 31-342, Poland*
[af] *Panjab University, Chandigarh 160014, India*
[ag] *Pennsylvania State University, University Park, PA 16802, United States*
[ah] *Institute of High Energy Physics, Protvino 142281, Russia*
[ai] *Purdue University, West Lafayette, IN 47907, United States*
[aj] *Pusan National University, Pusan 46241, Republic of Korea*
[ak] *Rice University, Houston, TX 77251, United States*
[al] *University of Science and Technology of China, Hefei, Anhui 230026, China*
[am] *Shandong University, Jinan, Shandong 250100, China*
[an] *Shanghai Institute of Applied Physics, Chinese Academy of Sciences, Shanghai 201800, China*
[ao] *State University of New York, Stony Brook, NY 11794, United States*
[ap] *Temple University, Philadelphia, PA 19122, United States*
[aq] *Texas A&M University, College Station, TX 77843, United States*
[ar] *University of Texas, Austin, TX 78712, United States*
[as] *University of Houston, Houston, TX 77204, United States*
[at] *Tsinghua University, Beijing 100084, China*

[au] *United States Naval Academy, Annapolis, MD 21402, United States*
[av] *Valparaiso University, Valparaiso, IN 46383, United States*
[aw] *Variable Energy Cyclotron Centre, Kolkata 700064, India*
[ax] *Warsaw University of Technology, Warsaw 00-661, Poland*
[ay] *Wayne State University, Detroit, MI 48201, United States*
[az] *World Laboratory for Cosmology and Particle Physics (WLCAPP), Cairo 11571, Egypt*
[ba] *Yale University, New Haven, CT 06520, United States*
[bb] *National Cheng Kung University, Tainan 70101, Taiwan*

ARTICLE INFO

ABSTRACT

Azimuthal correlations of charged hadrons with direct-photon (γ_{dir}) and neutral-pion (π^0) trigger particles are analyzed in central Au+Au and minimum-bias $p + p$ collisions at $\sqrt{s_{NN}} = 200$ GeV in the STAR experiment. The charged-hadron per-trigger yields at mid-rapidity from central Au+Au collisions are compared with $p + p$ collisions to quantify the suppression in Au+Au collisions. The suppression of the away-side associated-particle yields per γ_{dir} trigger is independent of the transverse momentum of the trigger particle (p_T^{trig}), whereas the suppression is smaller at low transverse momentum of the associated charged hadrons (p_T^{assoc}). Within uncertainty, similar levels of suppression are observed for γ_{dir} and π^0 triggers as a function of z_T ($\equiv p_T^{\text{assoc}}/p_T^{\text{trig}}$). The results are compared with energy-loss-inspired theoretical model predictions. Our studies support previous conclusions that the lost energy reappears predominantly at low transverse momentum, regardless of the trigger energy.

1. Introduction

Over the past decade, experiments at the Relativistic Heavy Ion Collider (RHIC) at BNL have studied the hot and dense medium created in heavy-ion collisions. The suppression of high-transverse momentum (p_T) inclusive hadrons [1–3], indicative of jet quenching, corroborates the conclusion that the medium created is opaque to colored energetic partons [4–7]. This phenomenon can be understood as a result of the medium-induced radiative energy loss of a hard-scattered parton as it traverses the Quark Gluon Plasma (QGP) created in heavy-ion collisions [8,9]. The angular correlation of charged hadrons with respect to a direct-photon (γ_{dir}) trigger was proposed as a promising probe to study the mechanisms of parton energy loss [10]. The presence of a "trigger" particle, having p_T greater than some selected value, serves as part of the selection criteria to analyze the event for a hard scattering. Direct photons are produced during the early stage of the collision, through leading-order pQCD processes such as quark–gluon Compton scattering ($qg \rightarrow q\gamma$) and quark–antiquark pair annihilation ($q\bar{q} \rightarrow g\gamma$). In these processes the transverse energy of the trigger photon approximates the initial p_T of the outgoing recoil parton, before the recoiling ("away-side") parton likely loses energy while traversing the medium and fragments into a jet. The jet-like yields associated with a trigger particle are estimated by integrating the correlated yields of charged hadrons over azimuthal distance from the trigger particle ($\Delta\phi$). Any suppression of the charged-hadron per-trigger yields in the away-side jets in central Au+Au collisions is then quantified by contrasting to the per-trigger yields measured in $p + p$ collisions, via the ratio of integrated yields, I_{AA} [11,12] (defined in Eq. (8)). When requiring a hadron trigger (such as a π^0), the p_T of the recoiling parton (and hence the away-side jet) is not as well approximated by the transverse energy of the trigger. For example, the PYTHIA Monte Carlo simulator [13] shows that, in $p + p$ collisions at $\sqrt{s_{NN}} = 200$ GeV, a π^0 trigger with $p_T > 12$ GeV/c carries, on average, only $80 \pm 5\%$ of the original scattered parton's p_T. This percentage from PYTHIA is consistent with the values extracted from this analysis, as described below.

Despite this complication, it is compelling to compare the suppression for γ_{dir} triggers with that for π^0 triggers because of the expected differences in geometrical biases at RHIC energies [14].

While the π^0 trigger is likely to have been produced near the surface of the medium, the γ_{dir} trigger does not suffer the same bias, since the photon mean free path is much larger than the size of the medium. Comparing γ_{dir}- and π^0-triggered yields offers further opportunities to explore the geometric biases and their interplay with parton energy loss. A next-to-leading order perturbative QCD calculation [15] suggests that production of hadrons at different z_T is also affected by different geometric biases, where $z_T \equiv p_T^{\text{assoc}}/p_T^{\text{trig}}$ (p_T^{assoc} and p_T^{trig} are transverse momenta of associated and triggered particles, respectively) represents the ratio of the transverse momentum carried by a charged hadron in the recoil jet to that of the trigger particle. The high-z_T hadrons in a jet recoiling from a γ_{dir} preferentially originate from a parton scattering near the away-side surface of the medium, since scatterings deeper in the medium will result in a stronger degradation of the high-momentum components of the jet. The high-z_T hadrons in a jet recoiling from a π^0 preferentially emerge from scatterings tangential to the surface from the already biased surface-dominated trigger jets (which is consistent with observations in [16]). These two mechanisms turn out to lead to the same level of suppression [15]. Only at low z_T does the full sampling of the volume by γ_{dir} triggers show a predicted difference from that of the surface-dominated π^0 triggers.

An additional effect at low z_T may be the redistribution of the parton's lost energy within the low-momentum jet fragments [17], which is not included in the calculation [15] described above. This was studied by the PHENIX Collaboration, which found an enhancement at low z_T and large angles, for direct photon triggers with p_T^{trig} in the range of 5–9 GeV/c at $\sqrt{s_{NN}} = 200$ GeV in the most central Au+Au collisions [11]. Enhancements due to this mechanism would be expected in hadrons recoiling from other triggers as well, such as π^0 or jets. A previous STAR measurement of hadrons associated with a reconstructed jet has shown an enhancement for $p_T < 2$ GeV/c, for two classes of jets with broadly separated energy scales, in which the enhancement at low p_T balances the suppression at high p_T [18].

Furthermore, leading order di-jet production comes from both quark and gluon jets. Recent calculations show that pions with high p_T relative to the total jet p_T are predominantly from quark jets [19,20], so, for the jet energies probed in this paper, the away-
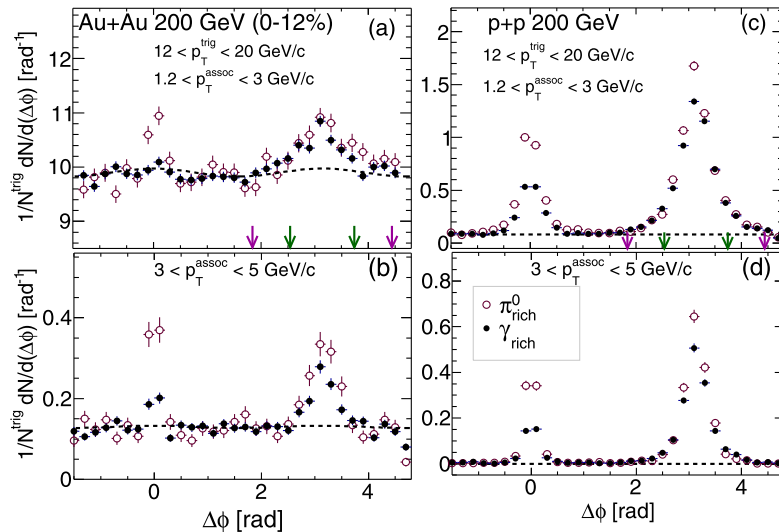
Fig. 1. (Color online.) The azimuthal correlation functions of charged hadrons per trigger for π^0_{rich} (open circles) and γ_{rich} (filled circles) triggers, measured in central (0–12%) Au+Au collisions and minimum-bias $p + p$ collisions. Panels (a) and (c) are for Au+Au and $p + p$ collisions, respectively, in $1.2 < p^{assoc}_T < 3$ GeV/c and panels (b) and (d) are that for $3 < p^{assoc}_T < 5$ GeV/c. The dashed curves indicate the background (charged hadrons not correlated with the jet), shown only for π^0_{rich} triggers, and the arrows indicate the range over which the away-side is integrated (green and violet colored arrows represent $|\Delta\phi - \pi| \leq 0.6$ and $|\Delta\phi - \pi| \leq 1.4$ respectively).

side mainly comes from gluon jets [21]. This is in contrast to the away-side of a γ_{dir} trigger, which mainly comes from quark jets, since at leading order a photon does not couple with a gluon. Thus it is expected that, on average, the away-side parton associated with a π^0 suffers more energy loss than that of a γ_{dir} due to the additional color factor from gluons. By comparing the suppression of away-side associated hadrons for γ_{dir} triggers to that for π^0 triggers, one can gain information about both the path-length and the color-factor dependence of parton energy loss.

This manuscript is organized as follows. The detector setup of the STAR experiment is discussed in Sec. 2. The transverse shower-shape analysis used to discriminate between π^0 and γ_{dir}, and the procedures to extract the charged-hadron spectra, associated with π^0 and γ_{dir} triggers, are discussed in Sec. 3. The per-trigger charged-hadron yields are presented as a function of z_T, in Sec. 4. The dependences of the suppression of these yields in central Au+Au collisions relative to those in minimum-bias $p + p$ collisions on both the trigger energy and the associated transverse momentum are discussed, with comparisons to theoretical model predictions. Finally, in Sec. 5, our observations are summarized.

2. Experimental setup

The data were taken by the Solenoidal Tracker at RHIC (STAR) experiment in 2011 and 2009 for Au+Au and $p + p$ collisions at $\sqrt{s_{NN}} = 200$ GeV, respectively. Using the Barrel Electromagnetic Calorimeter (BEMC) [22] to select events containing a high-p_T γ or π^0, the STAR experiment collected an integrated luminosity of 2.8 nb^{-1} of Au+Au collisions and 23 pb^{-1} of $p + p$ collisions. STAR provides 2π azimuthal coverage and wide pseudo-rapidity (η) coverage. The Time Projection Chamber (TPC) is the main charged-particle tracking detector [23], providing track information for the charged hadrons with $|\eta| < 1.0$. The centrality selection is determined from the charged-particle multiplicity in the TPC within $|\eta| < 0.5$. The BEMC is a sampling calorimeter, and each calorimeter module consists of a lead-scintillator structure and an embedded wire chamber, the Barrel Shower Maximum Detector (BSMD). The BSMD is situated approximately five radiation lengths from the front face of the BEMC. BEMC towers (each covering 0.05 units in η and ϕ) provide a measurement of the energy of electromagnetic clusters, whereas the BSMD, due to its high granularity (0.007

units in η and ϕ), provides high spatial resolution for the center of a cluster and the transverse development of the shower. Electromagnetic clusters are constructed from the response of one or two towers, depending on the location of the centroid as determined by the BSMD. The transverse extent of the shower is used to distinguish between γ_{dir} showers and decay photons from π^0. Details of the π^0/γ discrimination are discussed in the next section.

3. Analysis details

Events having a transverse energy in a BEMC cluster $E_T > 8$ GeV, with $|\eta| \leq 0.9$, are selected for this analysis. In order to distinguish a π^0, which at high p_T predominantly decays to two photons with a small opening angle, from a single-photon cluster, a transverse shower-shape analysis is performed. In this method, the overall BEMC cluster energy ($E_{cluster}$), the individual BSMD strip energies (e_i), and the distances of the strips (r_i) from the center of the cluster are used to construct the "Transverse Shower Profile" (TSP). The TSP is defined as, TSP $= E_{cluster}/\sum_i e_i r_i^{1.5}$ [12,24]. The π^0_{rich} (nearly pure sample of π^0) and γ_{rich} (enhanced fraction of γ_{dir}) samples are selected by requiring TSP < 0.08 and $0.2 <$ TSP < 0.6, respectively, in both $p + p$ and Au+Au collisions. The π^0_{rich} sample is estimated to be $\sim 95\%$ pure π^0, determined from studies of simulated π^0 and γ_{dir} embedded into real data. The $\Delta\phi$ azimuthal correlations are constructed with charged-hadron tracks within 1.2 GeV/c $< p^{assoc}_T < p^{trig}_T$ and $|\eta| < 1.0$. Both trigger samples are selected with $12 < p^{trig}_T < 20$ GeV/c (or $8 < p^{trig}_T < 20$ GeV/c for the study of the γ_{dir} p^{trig}_T dependence) and $|\eta| < 0.9$. There is an additional requirement that no track with momentum greater than 3 GeV/c is pointing to the trigger tower. This track-rejection cut prevents significant contamination of the measured BEMC energy of the trigger particle. The p_T threshold of the track-rejection cut was varied between 1 and 4 GeV/c, as a part of the systematic studies, and the variations showed no significant difference in the away-side charged-hadron yields.

The correlation functions represent the number of associated charged hadrons (N_{assoc}) per trigger particle, $(1/N_{trig})(dN_{assoc}/d\Delta\phi)$, as a function of $\Delta\phi$, where N_{trig} is the number of trigger particles. The yield is integrated over $\Delta\eta = 2$, with no correction applied for the particle-pair acceptance in $\Delta\eta$. In Fig. 1, a sample

of the azimuthal correlation functions for γ_{rich}- and π^0_{rich}-triggered associated charged hadrons, for different p_T^{assoc} ranges, is shown for the 12% most central Au+Au and minimum-bias $p + p$ collisions. In the lower p_T^{assoc} bins, the uncorrelated background (shown in Fig. 1 as dashed curves) is higher than that in higher p_T^{assoc} bins, especially in Au+Au collisions, whereas in $p + p$ collisions, this uncorrelated background is small in all p_T^{assoc} bins. On the near-side ($\Delta\phi \sim 0$) the π^0_{rich}-triggered correlated yields are larger than those for γ_{rich} triggers, as expected. The non-zero near-side γ_{rich}-triggered yields are due to the background in the γ_{rich} trigger sample and are used to determine the amount of background, as further discussed below. In the higher p_T^{assoc} range, it is also observed that the away-side ($\Delta\phi \sim \pi$) γ_{rich}-triggered yields are smaller than those of the π^0_{rich} triggers, which can be understood since the π^0 triggers originate from the fragmentation of partons generally having a higher energy than the corresponding direct-photon triggers.

The background subtraction and the pair-acceptance correction (in $\Delta\phi$) have been performed using a mixed-event technique (see *e.g.* [16]) for each z_T bin. Event mixing is performed among events having similar vertex position and centrality class. In Au+Au collisions, the background (*i.e.* what is not correlated with the jet) may still contain azimuthal correlations due to flow. The distributions of background pairs for different z_T bins are therefore modulated with the second Fourier (elliptic flow) coefficient (v_2) of the particle azimuthal distribution measured with respect to the event plane. It is given by B$[1 + 2\langle v_2^{trig}\rangle\langle v_2^{assoc}\rangle\cos(2\Delta\phi)]$, where B represents the level of background pairs and is determined assuming applicability of the "Zero-Yield at 1 radian" (ZYA1) method, a variation on the "Zero-Yield at Minimum" (ZYAM) method [25]. The $\langle v_2^{trig}\rangle$ ($\langle v_2^{assoc}\rangle$) is the average value of the second-order flow coefficient [26] of the trigger (associated) particle at the mean p_T^{trig} (p_T^{assoc}) in each z_T bin. The flow term in the background subtraction only has a significant effect for Au+Au collisions at low z_T, and the higher order flow components are ignored as their magnitudes are small in the most central Au+Au collisions. In $p + p$ collisions, B is determined assuming a flat (uncorrelated) background.

The trigger-associated charged-hadron yields are determined from the azimuthal correlation functions, per trigger particle (π^0_{rich} and γ_{rich} samples), per $\Delta\phi$, both on the near side ($\Delta\phi \sim 0$) and the away side ($\Delta\phi \sim \pi$). In this analysis, the near-side and away-side yields are extracted by integrating the correlation functions, for given z_T bins, over $|\Delta\phi| \leq 1.4$ and $|\Delta\phi - \pi| \leq 1.4$, respectively. The raw near-side and away-side associated charged-hadron yields are corrected for the associated-particle efficiencies determined by embedding simulated charged hadrons into real events. The average tracking efficiencies for charged hadrons (with $p_T^{assoc} > 1.2$ GeV/c) are determined via detector simulations to be around 70% and 90% for central Au+Au and minimum-bias $p + p$ collisions, respectively. The π^0-triggered yields are calculated from the π^0_{rich}-triggered correlation functions, with no further correction for the contamination in the trigger sample, because of the high purity in the π^0_{rich} sample.

Away-side charged-hadron yields for γ_{dir} triggers are determined by assuming zero near-side yield for γ_{dir} triggers, and using the following expression

$$Y_{\gamma_{dir}+h} = \frac{Y_{\gamma_{rich}+h}^{away} - R Y_{\pi^0_{rich}+h}^{away}}{1 - R}. \tag{1}$$

Here $Y_{\gamma_{rich}+h}^{away}$ ($Y_{\pi^0_{rich}+h}^{away}$) represents the away-side yield of γ_{rich} (π^0_{rich}), and R is given by

$$R = \frac{Y_{\gamma_{rich}+h}^{near}}{Y_{\pi^0_{rich}+h}^{near}}, \tag{2}$$

the ratio of the near-side yield in the γ_{rich}-triggered correlation function to the near-side yield in the π^0_{rich}-triggered correlation function. This means

$$1 - R = \frac{N^{\gamma_{dir}}}{N^{\gamma_{rich}}}, \tag{3}$$

where $N^{\gamma_{dir}}$ ($N^{\gamma_{rich}}$) is the number of γ_{dir} (γ_{rich}) triggers. The values of $1 - R$, representing the fractions of signal in the γ_{rich} trigger sample, are found to be 40% and 70% for $p + p$ and the central Au+Au collisions, respectively. Using this technique, almost all sources of background (including photons from asymmetric hadron decays and fragmentation photons) can be removed, assuming that their correlations are similar to those for π^0 triggers. This assumption was tested using PYTHIA simulations, with decay photons as the trigger particles, and it was found to be valid to within at least 15% (the statistical precision of the PYTHIA study).

Systematic uncertainties include the effects of track-quality selection criteria, neutral-cluster selection criteria, π^0/γ discrimination (TSP) cuts for the π^0_{rich} and γ_{rich} samples, the size of the ZYA1 normalization region, the v_2 uncertainty range, and the yield-integration windows. All of these sources of uncertainty are evaluated for each data point individually. For groups of sources that are not independent, such as different yield-extraction conditions, the maximum deviation among the different conditions is taken as the contribution to the systematic error. The systematic uncertainties from sources that are considered to be independent are added in quadrature. The π^0/γ discrimination uncertainty dominates in most z_T bins, varying between 10 and 25%. The track-quality selection criteria typically contributes a 5–10% uncertainty. In the lowest z_T bin in Au+Au collisions for π^0 triggers, the yield extraction uncertainty dominates with as much as 50% uncertainty in the near-side yield. The variation of the p_T threshold for the track-rejection cut for the neutral-tower trigger selection typically has a negligible effect.

4. Results and discussion

In this measurement, both π^0 and γ_{dir} triggers are required to be within a range of $12 < p_T^{trig} < 20$ GeV/c, or $8 < p_T^{trig} < 20$ GeV/c for the study of the p_T^{trig} dependence. In contrast to a γ_{dir} trigger, a π^0 trigger carries a fraction of the initial parton energy of the hard-scattered parton. In this case, the z_T for a trigger+associated-particle pair is only a loose approximation of the fractional parton energy carried by the jet constituent. The integrated away-side and near-side charged-hadron yields per π^0 trigger, $D(z_T)$, are plotted as a function of z_T, both for Au+Au (0–12% centrality) and $p + p$ collisions, in Fig. 2. Yields of the away-side associated charged hadrons are suppressed, in Au+Au relative to $p + p$, at all z_T except in the low z_T region. On the other hand, no suppression is observed on the near-side in Au+Au, relative to $p + p$ collisions, due to the surface bias imposed by triggering on a high-p_T π^0.

Fig. 3 shows the away-side $D(z_T)$ for γ_{dir} triggers, as extracted from Eq. (1), as a function of z_T for central Au+Au and minimum-bias $p + p$ collisions. The π^0-triggered away-side charged-hadron yields cannot be directly compared to those of γ_{dir} triggers, as the π^0 trigger is a fragment of a higher energy parton. One can approximate the fraction of additional energy by integrating z_T times a fit to the near-side $D(z_T)$ distribution, measured in $p + p$ collisions, over all z_T ($z_T = 0 \to \infty$). The value of that fraction is
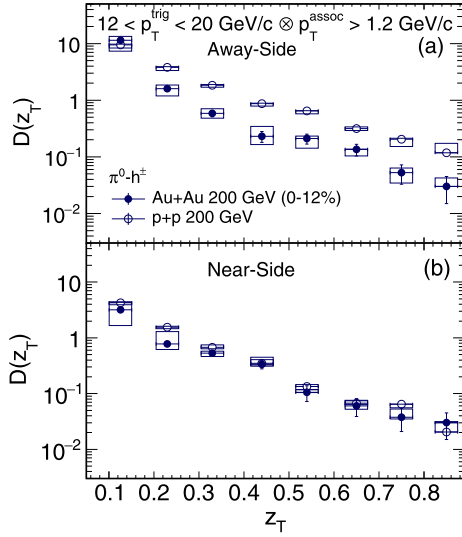
Fig. 2. (Color online.) The z_T dependence of π^0-$h^\pm$ away-side (a) and near-side (b) associated charged-hadron yields per trigger for Au+Au at 0–12% centrality (filled symbols) and $p + p$ (open symbols) collisions at $\sqrt{s_{NN}} = 200$ GeV. Vertical lines represent the statistical errors, and the vertical extent of the boxes represents systematic uncertainties.
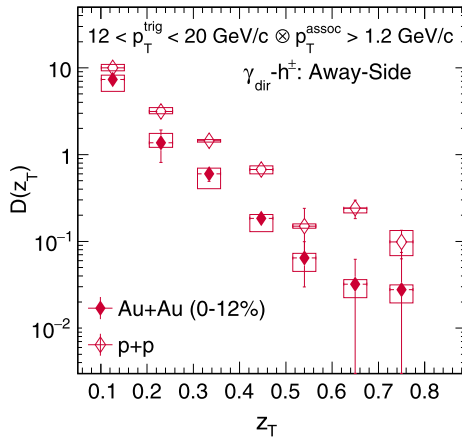

Fig. 3. (Color online.) The z_T dependence of γ_{dir}-$h^\pm$ away-side associated charged-hadron yields per trigger for Au+Au at 0–12% centrality (filled diamonds) and $p + p$ (open diamonds) collisions. Vertical lines represent statistical errors, and the vertical extent of the boxes represents systematic uncertainties.

$$\frac{\sum p_T^{assoc}}{p_T^{trig}} = 0.17 \pm 0.04. \tag{4}$$

From that, the fraction of energy carried by the π^0 trigger, with $p_T^{trig} = 12$–20 GeV/c, is estimated to be

$$\frac{p_T^{trig}}{p_T^{jet-charged}} = 85 \pm 3\%, \tag{5}$$

where $p_T^{jet-charged}$ is equal to the p_T^{trig} plus the total p_T carried by the near-side associated charged hadrons. This is consistent with what is obtained when applying the same analysis on π^0-triggered charged-hadron correlations from a PYTHIA simulation. In PYTHIA, the neutral associated energy can also be accounted for, giving us an estimate of the fractional energy carried by the π^0 trigger, when accounting for all associated particles (charged and neutral),

$$\frac{p_T^{trig}}{p_T^{jet}} = 80 \pm 5\%. \tag{6}$$
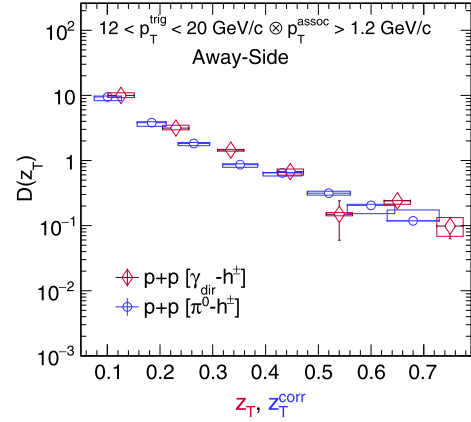

Fig. 4. (Color online.) The $z_T = p_T^{assoc}/p_T^{\gamma_{dir}}$ dependences of γ_{dir}-$h^\pm$ away-side associated charged-hadron yields per trigger for $p + p$ (open circles) collisions and that of $z_T^{corr} = p_T^{assoc}/p_T^{jet}$ dependence of the π^0-$h^\pm$ away-side associated charged-hadron yields (open diamonds) are shown. Vertical lines represent statistical errors bars, and the vertical extent of the boxes represents systematic uncertainties.

Applying this ratio as a correction factor to the z_T values of the away-side $D(z_T)$ for π^0 triggers in $p + p$ collisions results in the $D(z_T^{corr})$ distribution, where

$$z_T^{corr} = \frac{p_T^{assoc}}{p_T^{jet}}. \tag{7}$$

Since z_T^{corr} represents the fractional momentum of the jet carried by the associated particles, it is (to the extent that the p_T^γ is a good approximation of the initial p_T of the recoil parton) equivalent to the z_T measured when using γ_{dir} triggers. $D(z_T^{corr})$ is directly compared to the fragmentation function measured via direct-photon triggers in Fig. 4 and shows reasonable agreement.

In order to quantify the medium modification for γ_{dir}- and π^0-triggered recoil jet production as a function of z_T, the ratio, defined as

$$I_{AA} = \frac{D(z_T)^{AuAu}}{D(z_T)^{pp}}, \tag{8}$$

of the per-trigger conditional yields in Au+Au to those in $p + p$ collisions is calculated. In the absence of medium modifications, I_{AA} is expected to be equal to unity. Fig. 5 shows the away-side medium modification factor for π^0 triggers ($I_{AA}^{\pi^0}$) and γ_{dir} triggers ($I_{AA}^{\gamma_{dir}}$), as a function of z_T. $I_{AA}^{\pi^0}$ and $I_{AA}^{\gamma_{dir}}$ show similar suppression within uncertainties. At low z_T ($0.1 < z_T < 0.2$), both $I_{AA}^{\pi^0}$ and $I_{AA}^{\gamma_{dir}}$ show an indication of less suppression than at higher z_T. This observation is not significant in the z_T-dependence of I_{AA} because the uncertainties in the lowest z_T bin are large. However, when I_{AA} is plotted vs. p_T^{assoc} (shown in a later figure), the conclusion is supported with somewhat more significance. At high z_T, both $I_{AA}^{\pi^0}$ and $I_{AA}^{\gamma_{dir}}$ show a factor $\sim$ 3–5 suppression.

Theoretical model predictions, labeled as Qin [27] and ZOWW [15,28], using the same kinematic coverage for γ_{dir} triggered away-side charged-hadron yields, are compared to the data. In the model by Qin et al., the energy loss mechanism is incorporated into a thermalized medium for Au+Au collisions with impact parameters of 0–2.4 fm by using a full (3+1)-hydrodynamic evolution model description. Although this model also includes jet-medium photons (photons coming from the interaction of hard partons with the medium [29,30]) and fragmentation photons (photons radiating from hard partons [30]), both of these contribute to $I_{AA}^{\gamma_{dir}}$ mainly at high z_T and thus do not affect our comparison at low to mid z_T.
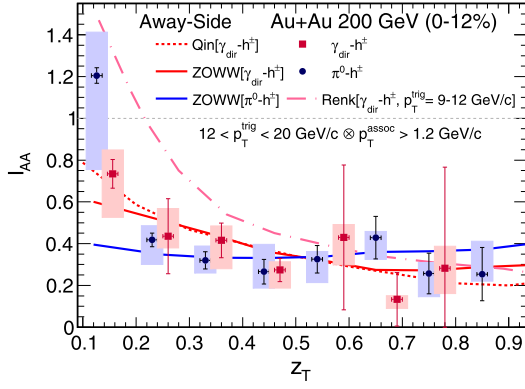
Fig. 5. (Color online.) The $I_{AA}^{\gamma_{dir}}$ (red squares) and $I_{AA}^{\pi^0}$ (blue circles) triggers are plotted as a function of z_T. The points for $I_{AA}^{\gamma_{dir}}$ are shifted by $+0.03$ in z_T for visibility. The vertical lines represent statistical error and the vertical extent of the boxes represents systematic errors. The curves represent theoretical model predictions [15,17, 27,28].
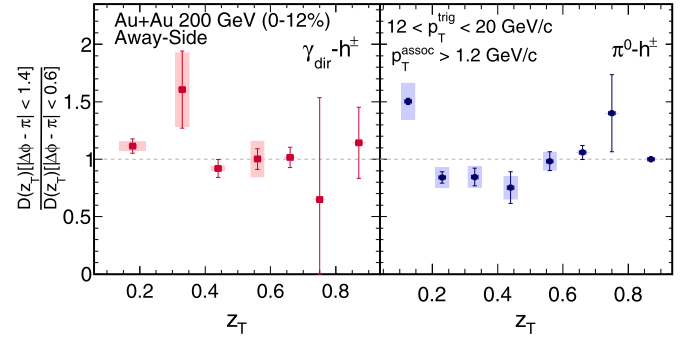

Fig. 6. (Color online.) The ratios of $D(z_T)$ obtained using an integration window of $|\Delta\phi - \pi| < 1.4$ radians over that of $|\Delta\phi - \pi| < 0.6$ radians for $\gamma_{dir} - h^\pm$ (left panel) and $\pi^0 - h^\pm$ (right panel), are plotted as a function of z_T for Au+Au at 0–12% central collisions. The vertical lines represent statistical error bars and boxes represent systematic errors. Since this is a ratio of yields for two overlapping angular windows, much of the uncertainties cancel; and only the surviving uncertainties are shown.
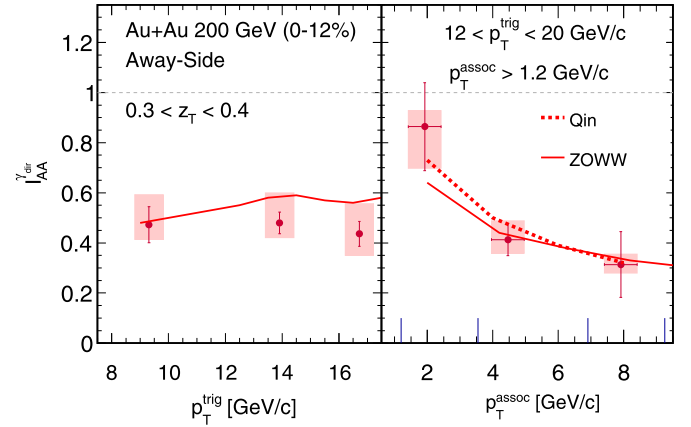
The calculation by ZOWW also incorporates the parameterized parton energy loss into a bulk-medium evolution [28]. It does not include fragmentation or jet-medium photons, and also describes the experimental measurement of $I_{AA}^{\gamma_{dir}}$ as a function of z_T for the top central Au+Au collisions. The calculated $I_{AA}^{\pi^0}$ (also by ZOWW) shows a somewhat larger suppression than the $I_{AA}^{\gamma_{dir}}$ at low z_T. The difference at low z_T between the $I_{AA}^{\gamma_{dir}}$ and the $I_{AA}^{\pi^0}$ (as calculated by ZOWW) is likely due to the color factor effect and the differences in average path lengths between π^0 triggers and γ_{dir} triggers. The calculated difference in the suppression is approximately 50% at $z_T = 0.1$. The data are not sensitive to this difference within the measured uncertainties. These models (Qin and ZOWW) do not include a redistribution of the lost energy to the lower p_T jet fragments, in contrast to the YaJEM model [17]. The YaJEM model is also shown in Fig. 5, although for a somewhat lower trigger p_T range of 9–12 GeV/c. It predicts $I_{AA}^{\gamma_{dir}} = 1$ at $z_T = 0.2$ (corresponding to $p_T^{assoc} \sim 1.8$ GeV/c) and rising well above 1 in the z_T range of 0.1–0.2 [17]. This is calculated with a small integration window of $\pi/5$ around $\Delta\phi = \pi$. Although this calculation has a different p_T^{trig} cut, such a large rise is not observed in our data. In contrast to the other calculations shown (Qin and ZOWW), the rise in $I_{AA}^{\gamma_{dir}}$ at low z_T in YaJEM is predominantly due to the redistribution of lost energy. In this picture, the in-medium shower is modified by the medium and a suppression at high z_T results in an enhancement at lower z_T. The authors compare the "medium-modified shower" picture to an "energy loss" picture, where the energy is carried through the medium by a single parton, and the lost energy would only show up at extremely low energies and large angles. In such a picture, they argue that the rise in $I_{AA}^{\gamma_{dir}}$ at low z_T would be more modest and $I_{AA}^{\gamma_{dir}}$ would remain less than 1.

Because PHENIX has reported an enhancement at low z_T ($z_T < 0.4$) in $I_{AA}^{\gamma_{dir}}$ at large angles [11], it is interesting to compare our results over the full integration window of $|\Delta\phi - \pi| < 1.4$ radians to an $I_{AA}^{\gamma_{dir}}$ calculated with a smaller window of $|\Delta\phi - \pi| < 0.6$ radians in Fig. 6. Within our uncertainties, an enhancement effect is only seen in the lowest z_T bin for π^0 triggers. However, for the PHENIX measurement, $z_T < 0.4$ corresponds to lower p_T for the associated hadrons ($\lesssim 2$ GeV/c), since the p_T^γ was chosen in the range of 5–9 GeV/c. In our analysis, associated hadrons with $p_T < 2$ GeV/c are only present at $z_T < 0.2$. The apparent inconsistency between STAR and PHENIX, when investigating the recovery of the lost energy as a function of z_T, indicates that p_T^{assoc} may be the more pertinent variable. The conclusion is that the "modified

Fig. 7. (Color online.) The values of $I_{AA}^{\gamma_{dir}}$ are plotted as a function of p_T^{trig} (left panel) and p_T^{assoc} (right panel). The vertical line and shaded boxes represent statistical and systematic errors, respectively. The curves represent model predictions [15,27,28].

fragmentation function" (constructed from the in-medium jet-like yields as a function of z_T) is not universal. In particular, the lost energy is not recovered at a fixed range of z_T, but perhaps at a given range of p_T^{assoc}. The conclusion that the lost energy is recovered at larger angles only for $p_T < 2$ GeV/c, regardless of the trigger energy, is consistent with the conclusion of the STAR paper on jet-hadron correlations [18].

The earlier measurements [12] at low trigger energy ($8 < p_T^{trig} < 16$ GeV/c) show the same level of suppression (factor 3–5) via the medium modification factor ($I_{AA}^{\pi^0}$ and $I_{AA}^{\gamma_{dir}}$) down to $z_T \sim 0.3$. This suggests that I_{AA} does not depend on the trigger energy at mid to high z_T for γ_{dir} and π^0-triggered away-side jets with trigger p_T ranging from 8 to 20 GeV/c. This is further investigated in Fig. 7 with γ_{dir} triggers, since the photon trigger energy closely approximates the initial outgoing parton energy. The left panel shows $I_{AA}^{\gamma_{dir}}$ as a function of p_T^{trig}, for $0.3 < z_T < 0.4$. The per-trigger nuclear modification factor of γ_{dir}-triggered away-side charged-hadron yields is independent of the trigger energy of the γ_{dir} within our 25% systematic uncertainty. This indicates that the away-side parton energy loss is not sensitive to the initial parton energy in this range of 8–20 GeV/c, as measured with our level of precision. The ZOWW calculation also predicts $I_{AA}^{\gamma_{dir}}$ as a function of p_T^{trig} to be approximately flat in this range. In the right panel, the values of $I_{AA}^{\gamma_{dir}}$ are plotted as function of p_T^{assoc}. It shows that the low-p_T^{assoc} hadrons on the away-side are not as suppressed as

those at high p_T^{assoc}. Both model predictions shown [15,27], which do not include the redistribution of lost energy, are in agreement with the data.

5. Summary

In summary, in order to understand the medium modification of partons in the QGP, away-side charged-hadron yields for γ_{dir} and π^0 triggers in central (0–12%) Au+Au collisions are compared with those in minimum-bias $p + p$ collisions. Both $I_{AA}^{\pi^0}$ and $I_{AA}^{\gamma_{dir}}$ show similar levels of suppression, with the expected differences due to the color-factor effect and the path-length dependence not manifesting themselves within experimental uncertainties. At low z_T and low p_T^{assoc}, the data are consistent with less suppression than at higher p_T^{assoc}. The suppression shows little difference for integration windows of $\pm$ 0.6 vs. $\pm$ 1.4 radians around $\Delta\phi = \pi$, with an enhancement at large angles observed only for $z_T < 0.2$ ($p_T^{\text{assoc}} < 2.4$ GeV/c) for π^0 triggers. There is no trigger-energy dependence observed in the suppression of γ_{dir}-triggered yields, suggesting little dependence for energy loss on the initial parton energy, in the range of $p_T^{\text{trig}} = 8$–20 GeV/c. The data are consistent with model calculations [15,27,28], in which the suppression is caused by parton energy loss in a thermalized medium. These calculations do not include redistribution of energy within the shower. The very large $I_{AA}^{\gamma_{dir}}$ at low z_T predicted by models of in-medium shower modification (including energy redistribution) [17] is not observed for $p_T^{\text{trig}} > 12$ GeV/c. This is in contrast to the PHENIX result [11], where the $I_{AA}^{\gamma_{dir}}$ exceeds unity, for p_T^{trig} 5–9 GeV/c. However, it is not clear that the redistribution of lost energy would scale with the jet energy. In fact, our studies support previous conclusions that the lost energy reappears predominantly at low p_T (approximately $p_T < 2$ GeV/c), regardless of the trigger p_T. This leads to the important conclusion that the modified fragmentation function is not universal (*i.e.* it does not have the same z_T dependence for all trigger p_T).

Acknowledgments

References

[1] K. Adcox, et al., PHENIX Collaboration, Phys. Rev. Lett. 88 (2001) 022301.
[2] C. Adler, et al., STAR Collaboration, Phys. Rev. Lett. 89 (2002) 202301.
[3] C. Adler, et al., STAR Collaboration, Phys. Rev. Lett. 90 (2003) 082302.
[4] J. Adams, et al., STAR Collaboration, Nucl. Phys. A 757 (2005) 102.
[5] K. Adcox, et al., PHENIX Collaboration, Nucl. Phys. A 757 (2005) 184.
[6] B.B. Back, et al., PHOBOS Collaboration, Nucl. Phys. A 757 (2005) 28.
[7] I. Arsene, et al., BRAHMS Collaboration, Nucl. Phys. A 757 (2005) 1.
[8] M. Gyulassy, P. Levai, I. Vitev, Phys. Rev. Lett. 85 (2000) 5535.
[9] M. Gyulassy, P. Levai, I. Vitev, Phys. Lett. B 538 (2002) 282.
[10] X.-N. Wang, Z. Huang, I. Sarcevic, Phys. Rev. Lett. 77 (1996) 231.
[11] A. Adare, et al., PHENIX Collaboration, Phys. Rev. Lett. 111 (2013) 032301.
[12] B.I. Abelev, et al., STAR Collaboration, Phys. Rev. C 82 (2010) 034909.
[13] T. Sjöstrand, S. Mrenna, P. Skands, Comput. Phys. Commun. 178 (2008) 852 (Default parameters in PYTHIA 8.185, phaseSpace: pTHatMin = 4).
[14] T. Renk, Phys. Rev. C 74 (2006) 034906.
[15] H. Zhang, J.F. Owens, E. Wang, X.-N. Wang, Phys. Rev. Lett. 103 (2009) 032302.
[16] L. Adamczyk, et al., STAR Collaboration, Phys. Rev. C 87 (2013) 044903.
[17] T. Renk, Phys. Rev. C 80 (2009) 014901.
[18] L. Adamczyk, et al., STAR Collaboration, Phys. Rev. Lett. 112 (2014) 122301.
[19] D. de Florian, R. Sassot, M. Epele, R.J. Hernandez-Pinto, M. Stratmann, Phys. Rev. D 91 (2015) 014035.
[20] T. Kaufmann, A. Mukherjee, W. Vogelsang, Phys. Rev. D 92 (2015) 054015.
[21] D. de Florian, R. Sassot, M. Stratmann, Phys. Rev. D 75 (2007) 114010.
[22] M. Beddo, et al., Nucl. Instrum. Methods A 499 (2003) 725.
[23] M. Anderson, et al., Nucl. Instrum. Methods A 499 (2003) 659.
[24] N.R. Sahoo, for the STAR Collaboration, arXiv:1512.08782 [nucl-ex].
[25] N.N. Ajitanand, et al., Phys. Rev. C 72 (2005) 011902.
[26] J. Adams, et al., STAR Collaboration, Phys. Rev. C 72 (2005) 014904.
[27] G.-Y. Qin, J. Ruppert, C. Gale, S. Jeon, G.D. Moore, Phys. Rev. C 80 (2009) 054909.
[28] X.-F. Chen, C. Greiner, E. Wang, X.-N. Wang, Z. Xu, Phys. Rev. C 81 (2010) 064908;
X.-N. Wang, private communication.
[29] T. Renk, Phys. Rev. C 88 (2013) 034902.
[30] S. De, R.J. Fries, D.K. Srivastava, Phys. Rev. C 90 (2014) 034911.